

AN UNUSUAL QUADRUPLE SYSTEM  $\xi$  TAURI

J. A. Nemravová<sup>1</sup>, P. Harmanec<sup>1</sup>, J. Bencheikh<sup>2</sup>, C. T. Bolton<sup>3</sup>,  
 H. Božić<sup>4</sup>, M. Brož<sup>1</sup>, S. Engle<sup>5</sup>, J. Grunhut<sup>6</sup>, E. F. Guinan<sup>5</sup>, C. A. Hummel<sup>7</sup>,  
 D. Korčáková<sup>1</sup>, P. Koubský<sup>8</sup>, P. Mayer<sup>1</sup>, D. Mourard<sup>2</sup>, J. Ribeiro<sup>9</sup>,  
 M. Šlechta<sup>8</sup>, D. Vokrouhlický<sup>1</sup>, V. Votruba<sup>8</sup>, M. Wolf<sup>1</sup>, P. Zasche<sup>1</sup>,  
 the CHARA/VEGA and the NPOI teams.

<sup>1</sup>*Astronomical Institute, Faculty of Mathematics and Physics, Charles University in Prague,  
 V Holešovičkách 2, Praha 8, Czech Republic.*

<sup>2</sup>*Laboratoire Lagrange, OCA/UNS/CNRS UMR7293,  
 BP4229, 06304 Nice Cedex*

<sup>3</sup>*David Dunlap Observatory, University of Toronto,  
 Richmond Hill, Canada.*

<sup>4</sup>*Hvar Observatory, Faculty of Geodesy,  
 Kačićeva 26, Zagreb, Croatia.*

<sup>5</sup>*Department of Astronomy & Astrophysics, Villanova University,  
 800 Lancaster Ave. Villanova, PA 19085, USA.*

<sup>6</sup>*Department of Physics, Engineering Physics & Astronomy, Queens University,  
 Kingston, Ontario, Canada.*

<sup>7</sup>*European Southern Observatory,  
 Karl-Schwarzschild-Str. 2, 85748 Garching bei München, Germany.*

<sup>8</sup>*Astronomical Institute of the Academy of Sciences,  
 Ondřejov, Czech Republic.*

<sup>9</sup>*Observatório do Instituto Geográfico do Exército,  
 R. Venezuela, Lisboa, Portugal.*

**Abstract.** A preliminary analysis of spectroscopic, photometric and interferometric observations of the triple subsystem of a hierarchical quadruple system  $\xi$  Tau is presented. The triple system consists of a close eclipsing binary ( $P^A = 7^d.146651$ ), revolving around a common centre of gravity with a distant tertiary ( $P^B = 145^d.17$ ). All three stars have comparable brightness. The eclipsing pair consists of two slowly-rotating A stars while the tertiary is a rapidly-rotating B star. The outer orbit is eccentric ( $e^B = 0.237 \pm 0.022$ ). Available electronic radial velocities indicate an apsidal advance of the outer orbit with a period  $P_{\text{APS}}^B = 224 \pm 147$  yr.

**Key words:** stars: binary stars, stars: hot stars

## 1. Introduction

$\xi$  Tau (2 Tau, HD 21364, HIP 16083, HR 1038) is a hierarchical quadruple system, consisting of sharp-lined A stars, undergoing binary eclipses, a more distant broad-lined B star and a much more distant (the semi-major axis  $a^C = 0''441 \pm 0''027$ , Rica Romero 2010) F star. Here, we shall denote the components as follows: C (F-type), B (B-type), Aa, Ab (A-types) and the orbits: C (F-type), B (B-type), A (A-types). The visual magnitude of  $\xi$  Tau ( $V = 3^m72$ ) and its declination  $9^\circ44'$  make it an easy target for a wide range of instruments and observational techniques. The binary nature of the system was discovered by Campbell (1909). The outermost orbit C was resolved using speckle-interferometry by Mason et al. (1999). All speckle-interferometric observations of the system were analysed by Rica Romero (2010), who found an orbital period  $P^C = 52 \pm 15$  yrs. The orbital elements of the triple subsystem were published by Bolton and Grunhut (2007). The Hipparcos parallax of the system is  $p = 15.6 \pm 1.04$  mas (van Leeuwen, 2007a,b). As we were unable to detect either spectral or light variations of the distant and faint F component, we do not deal with the orbit C in this study.

## 2. Observations and data reduction

We have collected a rich series of spectroscopic, photometric and interferometric observations spanning more than two decades.

### 2.1. SPECTROSCOPY

The 131 electronic slit spectra cover time interval RJD = 49300 to 55971<sup>1</sup>. They were secured at three observatories: 1) Ondřejov Observatory, Czech Republic, 2) David Dunlap Observatory, Canada, and 3) Observatory of the Army Geographic Institute, Portugal.

Spectral lines of the three components are visible in the spectra. We studied the  $H\gamma$ ,  $H\beta$ , and  $H\alpha$  Balmer lines and also stronger metallic lines (Mg II 4481 Å, Si II 6347 Å and Si II 6371 Å), in which the contribution of the A-type stars is dominant. The B-type component contributes about 60 % to the total flux in the optical region and its spectral lines are significantly

---

<sup>1</sup>RJD = JD - 2400000

rotationally broadened ( $v_R \sin i \geq 200 \text{ km s}^{-1}$ ). The spectral lines of both A-type stars are sharp and very similar to each other.

## 2.2. PHOTOMETRY

Altogether, 1786 *UBV* observations (spanning RJD = 54116 to 55956) were secured at three observatories: 1) Hvar Observatory, Croatia, 2) South African Astronomical Observatory, South Africa, and 3) Villanova APT, USA. We also used 69 Hipparcos  $H_p$  observations (Perryman and ESA, 1997) spanning RJD = 47909 to 48695. These were transformed to the Johnson *V* using a formula found by Harmanec (1998). The light curve of the system, which is shown in Fig. 3, shows shallow and narrow primary and secondary minima of comparable depth of 0.12 mag in the Johnson *V* filter.

## 2.3. SPECTRO-INTERFEROMETRY

The  $\xi$  Tau system was observed with the NPOI interferometer between 1991 and 2012, the bulk of observations being taken during the last decade, and also with the VEGA/CHARA spectro-interferometer in 2011 and 2012.<sup>2</sup>

# 3. Data analysis and preliminary results

## 3.1. ORBITAL SOLUTION

We measured RVs by an automatic comparison of suitably chosen synthetic and observed spectra. The measurements were then divided into two subsets well-separated in time from each other. We used program FOTEL Hadrava (2004a) (release on the 25<sup>th</sup> of June, 2003) to compute the orbital solution. This release of the program does not allow modelling of apsidal motion for the outer orbit. Therefore the RVs measured on the A-type stars had to be fitted on each subset separately. This does not apply to the RVs of the B-type star. This component can be considered moving in a binary system and its apsidal motion can be treated properly in FOTEL.

Elements published by Bolton and Grunhut (2007) were used as an initial estimate. The orbital period of the inner orbit  $P^A$  was kept fixed at the value given by the light curve solution (see below). The orbital

---

<sup>2</sup>Only observations from 2011 being reported here.

**Table I:** The orbital solution resulting from spectral-disentangling of the spectroscopic observations, where  $P_S$  denotes the sidereal orbital period,  $P_{An}$  anomalistic orbital period,  $T_P$  the epoch of periastron,  $e$  the eccentricity,  $\omega$  the longitude of periastron,  $K_1$  the semi-amplitude,  $q$  the mass ratio, and  $P_{APS}$  the period of the apsidal advance.

Element	Outer orbit (B)	Inner orbit (A)
$P_{An}$ (d)	$145.44 \pm 0.10$	–
$P_S$ (d)	$145.17 \pm 0.10$	$7.146651 \pm 0.000010$
$T_P$ (RJD)	$55609.88 \pm 0.01$	–
$T_{conj.}$ (RJD)	$55580.77 \pm 0.01$	$48299.075 \pm 0.010$
$e$	$0.22 \pm 0.15$	$0.0 + 0.05$
$\omega$ (deg)	$189.7 \pm 5.0$	$90 \pm 10$
$P_{APS}^B$ yr	$214 \pm 100$	–
$K_1$ (km s $^{-1}$ )	$38.02 \pm 5.0$	$89.1 \pm 10.0$
$q$	$1.01 \pm 0.20$	$0.96 \pm 0.10$

elements corresponding to the best-fit of the RVs measured on the lines of the B-type star are: the anomalistic period  $P_{an}^B = 145.42 \pm 0.15$  d, the periastron epoch  $T_P^B$  (RJD) =  $55608.9 \pm 2.3$ , the eccentricity  $e^B = 0.237 \pm 0.022$ , the periastron longitude  $\omega^B = 187.0 \pm 6.9$  deg, and semi-amplitude  $K_1^B = 38.44 \pm 0.90$  km s $^{-1}$ . The results also revealed presence of an apsidal motion of the orbit B with a period of  $P_{APS}^B = 224 \pm 147$  yrs. The RV curve of the tertiary and the best-fit model are shown in Fig. 1.

The spectral-disentangling program KOREL (Hadrava, 2004b) was used for the final orbital solution and the corresponding orbital elements are listed in Tab. I. The disentangled component spectra are shown in Fig. 2.

### 3.2. LIGHT-CURVE SOLUTION

We used the program PHOEBE (Prša and Zwitter, 2005) for modelling of the brightness variations of  $\xi$  Tau. The limb-darkening coefficients were taken from Claret (2000). The semi-major axis and the mass ratio obtained with spectral-disentangling were kept fixed. The light contribution of the B-type star had to be considered as the third light, its relative luminosity in the V band being  $L_r^V = 0.60 \pm 0.02$ . As the secondary minimum occurs a bit earlier than half of the period after the primary one, we had to allow for a small orbital eccentricity. The elements of the solution are presented

AN UNUSUAL QUADRUPLE SYSTEM  $\xi$  TAURI

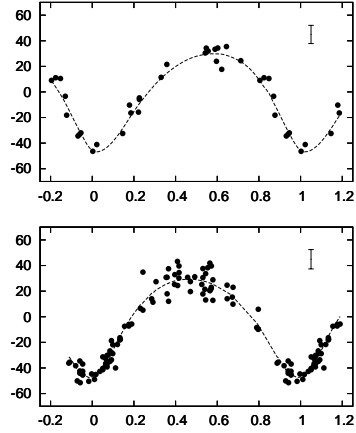


Figure 1: A secular evolution of the orbit B. The RVs measured on the spectral lines of the B-type star in between: upper panel: RJD = 49300 to 50500 and lower panel: RJD = 55560 to 55981. The mean RV curve of the time interval is shown with dashed line. The typical uncertainty of one measurement is denoted by line segments.

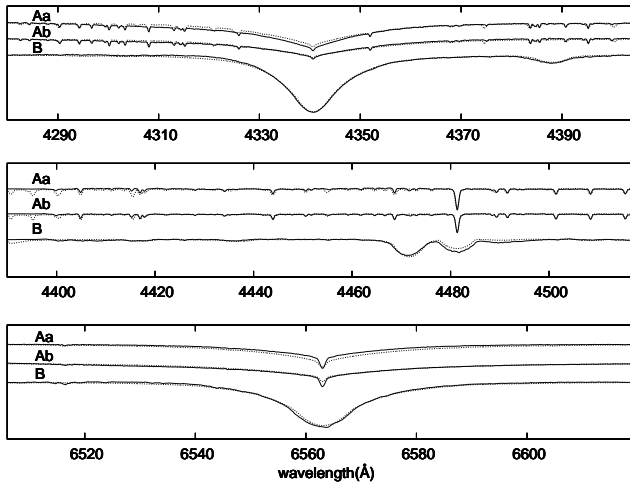


Figure 2: Spectra of the triple subsystem components obtained by means of disentangling (full line) and synthetic spectra fitted to the disentangled ones (dotted line). With the exception of the spectrum covering wavelength interval  $\Delta\lambda = 4390 - 4518 \text{ \AA}$  all disentangled spectra did not have perfectly flat continua and we had to re-normalize them.

in Tab. II.

### 3.3. INTERFEROMETRIC SOLUTION

Interferometric observations were fitted in Fourier space in order to obtain positions of the stars. Then the positions of stars were fitted in order to obtain the orbital properties. Results are presented in Tab. III. In case of the VEGA/CHARA interferometer, the spectroscopic solution presented in this paper was used to obtain an initial model of the system for the modelling of the star positions. NPOI interferometer is unable to resolve the inner system.

### 3.4. COMPARISON OF THE OBSERVED AND SYNTHETIC SPECTRA

We have used a program, which interpolates in grids of synthetic spectra and compares the synthetic spectrum to observed ones using the least-square method. The elements, which can be optimized, are: the effective temperature  $T_{\text{eff}}$ , the logarithm of gravitational acceleration  $\log g$ , the projected rotational velocity  $v_{\text{R}} \sin i$ , the relative luminosity  $L_{\text{R}}$ , and the radial velocities of the components  $RV_i$ . The grids of synthetic spectra by Lanz and Hubený (2003, 2007), and Palacios et al. (2010) were used. The best-fit synthetic spectra are shown in Fig. 2 and the corresponding optimal parameters are in Tab. IV.

## 4. Discussion

### 4.1. DERIVED PROPERTIES OF THE SYSTEM

An estimated precision of the RV measurements on the electronic spectra is approximately  $2 \text{ km s}^{-1}$  for the A-type stars and  $5 \text{ km s}^{-1}$  for the B-type star. A good phase coverage for both orbital periods led to reliable RV-curve solutions with FOTEL (giving the rms error of one observation  $\leq 7 \text{ km s}^{-1}$ ). The FOTEL orbital elements provided good initial values for the final solution with KOREL. We mapped  $\chi^2$  around the minimum of the sum of squares in order to get estimates of the uncertainties of the elements. We did only basic uncertainty analysis and the uncertainties given in the Tab. I were estimated on basis of the above-mentioned maps.

**Table II:** Light curve solution for the inner orbit of  $\xi$  Tau.  $P$  denotes the orbital period,  $T_{\min}$  the epoch of the primary light curve minimum,  $i$  the orbital inclination,  $e$  the eccentricity,  $\omega$  the periastron longitude,  $r$  the radius,  $T_{\text{eff}}$  the effective temperature and  $L_r^V$  the relative brightness in the Johnson V-band.

Orbital properties		
Parameters	Values	
$P^A$ (d)	$7.146656 \pm 0.000020$	
$T_{\min}^A$ (RJD)	$48302.6374 \pm 0.0010$	
$i^A$ (deg)	$86.2 \pm 0.5$	
$e^A$	$0.016 \pm 0.010$	
$\omega^A$ (deg)	$110 \pm 10$	
Properties of the close binary components		
Parameters	Aa	Ab
$r$ ( $R_{\odot}$ )	$2.0 \pm 0.2$	$1.5 \pm 0.2$
$T_{\text{eff}}$ (K)	$9250 \pm 100$	9200(fixed)*
$L_r^V$	$0.26 \pm 0.02$	$0.14 \pm 0.02$

\*Taken from the fit of the disentangled spectra to the synthetic ones.

**Table III:** List of the best-fit interferometric orbital elements.  $T_p$  denotes the periastron epoch,  $P_S$  the sidereal orbital period,  $i$  the inclination,  $\Omega$  the longitude of the ascending node,  $e$  the eccentricity,  $\omega$  the periastron longitude,  $a$  the angular size of the semi-major axis,  $P_{\text{APS}}$  the period of the apsidal motion,  $N$  the number of the interferometric observations.

Element	Instrument		
	VEGA/CHARA		NPOI
$T_p$ (RJD)**	$55755.04 \pm 0.1$		$53712.90 \pm 0.34$
$N$	5		22
	Inner Orbit (A)	Outer Orbit (B)	Outer Orbit (B)
$P_S$	7.146656(fixed)	145.17(fixed)	$145.12 \pm 0.055$
$i$ (deg)	$97.5 \pm 5.0$	$85.0 \pm 4.0$	$87.07 \pm 0.19$
$\Omega$ (deg)*	$350.5 \pm 4.0$	$329.2 \pm 2.0$	$328.63 \pm 0.38$
$e$	–	$0.24 \pm 0.04$	$0.213 \pm 0.007$
$\omega$ (deg)	–	$182.0 \pm 5.0$	$163.07 \pm 0.13$
$a$ (mas)	–	$15.5 \pm 0.4$	$16.09 \pm 0.18$
$P_{\text{APS}}^B$ yr	–	–	$266 \pm 65$

\*Values of  $\Omega + 180^\circ$  are also possible.\*\* $T_p$  denotes reference epoch in case of the inner orbit.

**Table IV:** The Result of the observed spectra fitting to the synthetic spectra.  $T_{\text{eff}}$  denotes the effective temperature,  $\log g$  the logarithm of gravitational acceleration,  $v_{\text{R}} \sin i$  the projected rotational velocity,  $L_{\text{r}}$  the relative luminosity,  $RV_{\gamma}$  the systemic radial velocity and  $Z$  the metallicity.  $\Delta\lambda \in [4380, 4500] \text{ \AA}$  region was fitted.

Parameter	System component		
	B	Aa	Ab
$T_{\text{eff}}$ (K)	$15100 \pm 200$	$9400 \pm 500$	$9200 \pm 500$
$\log(g)_{\text{[cgs]}}$	$4.3 \pm 0.1$	4.2(fixed)	4.2(fixed)
$v_{\text{R}} \sin i$ (km s $^{-1}$ )	$246 \pm 10$	$33 \pm 2$	$34 \pm 2$
$L_{\text{r}}$	$0.73 \pm 0.02$	$0.14 \pm 0.02$	$0.13 \pm 0.02$
$RV_{\gamma}$ (km s $^{-1}$ )	$2.4 \pm 5.0$	$7.7 \pm 5.0$	$6.9 \pm 5.0$
$Z$ ( $Z_{\odot}$ )	2(fixed)	2(fixed)	2(fixed)

The light curve solution exhibits a high degeneracy in the diameters of the stars. This is due to a very shallow and almost identical eclipse minima. The light curve solution also indicates a small eccentricity of the orbit A  $e^{\text{A}} \leq 0.03$ . The mutual interaction between the close binary A and the tertiary should also cause a secular nodal motion. If the orbits are not coplanar, the depths of the eclipses should change in the course of time. We compared observations from two seasons, but we cannot confirm such an effect yet. Data from more epochs are needed.

The orbital solutions based on the interferometric observations from the CHARA/VEGA (which depend heavily on the spectroscopic solution in Tab. I) and the NPOI do not agree with each other in the longitude of periastron. The value of longitude of periastron based on the ephemeris obtained on the NPOI data would be  $\omega^{\text{B}}(RJD = 55755) = 171 \pm 2$  deg. However, the discrepancy may result from underestimation of the uncertainties of the NPOI fit, because only preliminary uncertainty analysis was done.

The combined orbital elements of the inner orbit imply masses of the components of the system:  $M^{\text{Aa}} = 2.29 \pm 0.91 M_{\odot}$ ,  $M^{\text{Ab}} = 2.20 \pm 0.78 M_{\odot}$ ,  $M^{\text{B}} = 4.53 \pm 1.51 M_{\odot}$  and semi-major axii of the orbits:  $a^{\text{A}} = 25.77 \pm 3.95 R_{\odot}$  and  $a^{\text{B}} = 213 \pm 51 R_{\odot}$ , while the combined orbital elements of the outer orbit leads to masses:  $M^{\text{B}} = 3.08 \pm 1.24 M_{\odot}$ ,  $M^{\text{Aa+Ab}} = 3.11 \pm 0.65 M_{\odot}$ . Although both results agree with each other within uncertainty boxes, the difference between the expected values might suggest



discrepancy in our model of the triple subsystem.

#### 4.2. APSIDAL MOTION

The detected apsidal motion is most likely caused by an interaction between the pair of the A-type stars and the B-type star. The large semi-major axis of the orbit B  $a^B = 213 \pm 51 R_\odot$  and the relatively low eccentricity  $e^B = 0.2 \pm 0.15$  exclude a possibility that the apsidal advance would be caused either by the stellar internal structure or by a relativistic effect.

We calculated the periods of the apsidal motion  $P_B^{\text{APS}} \in [142, 352]$  yr and the nodal motion  $P^{\text{NOD}} \in [16, 24]$  yr with the formulæ derived by Soderhjelm (1975) and independently by a direct integration of Lagrange equations (high uncertainty in the mass ratio  $q^B$  was taken into account). These intervals of periods are possible (from the point of view of dynamics) if our model of the system given by the spectroscopic solution is correct. Both intervals of periods depend on the angle between the orbital planes. Values of the angle in the range  $j \in [0, 35]$  were evaluated.

### 5. Future plans and expectations

The ultimate goal of our effort will be the determination of very accurate masses and radii of all components and of dynamical properties and possible evolution of the system. We plan to obtain additional high-precision light curve of the eclipsing pair with the MOST satellite, and continue observations with the VEGA/CHARA interferometer as well as ground-based photometric and spectroscopic observations.

### Acknowledgements

The Czech authors were supported by the grants No. 703812 (PH and JN) of the Grant Agency of the Charles University in Prague and P209/10/0715 (PH, PM, JN, MW, PZ) of the Czech Science Foundation as well as from the Research programs MSM0021620860 (MB, PH, DV, PM, MW, PZ) and AV0Z10030501 (PK, VV, MŠ).

## References

- Bolton, C. T., and Grunhut, J. H.: 2007, in W. I. Hartkopf, E. F. Guinan, and P. Harmanec (eds), *IAU Symposium*, Vol. 240 of *IAU Symposium*, p. 66.
- Campbell, W. W.: 1909, *Astrophys. J.* **29**, 224–228.
- Claret, A.: 2000, *Astron. Astrophys.* **363**, 1081–1190.
- Hadrava, P.: 2004a, *Publ. Astron. Inst. Acad. Sci. Czech Rep.* **92**, 1–14.
- Hadrava, P.: 2004b, *Publ. Astron. Inst. Acad. Sci. Czech Rep.* **92**, 15–35.
- Harmanec, P.: 1998, *Astron. Astrophys.* **335**, 173–178.
- Lanz, T., and Hubený, I.: 2003, *Astrophys. J., Suppl. Ser.* **146**, 417–441.
- Lanz, T., and Hubený, I.: 2007, *Astrophys. J., Suppl. Ser.* **169**, 83–104.
- Mason, B. D., Martin, C., Hartkopf, W. I., Barry, D. J., Germain, M. E., Douglass, G. G., Worley, C. E., Wycoff, G. L., ten Brummelaar, T., and Franz, O. G.: 1999, *Astron. J.* **117**, 1890–1904.
- Palacios, A., Gebran, M., Josselin, E., Martins, F., Plez, B., Belmas, M., and Lèbre, A.: 2010, *Astron. Astrophys.* **516**, A13.
- Perryman, M. A. C., and ESA: 1997, *The HIPPARCOS and TYCHO catalogues*, ESA SP Series 1200, Noordwijk, Netherlands.
- Prša, A., and Zwitter, T.: 2005, *Astrophys. J.* **628**, 426–438.
- Rica Romero, F. M.: 2010, *Rev. Mex. Astron. Astrofis.* **46**, 263–277.
- Soderhjelm, S.: 1975, *Astron. Astrophys.* **42**, 229–236.
- van Leeuwen, F.: 2007a, in F. van Leeuwen (ed.), *Astrophysics and Space Science Library*, Vol. 350, Springer, Germany.
- van Leeuwen, F.: 2007b, *Astron. Astrophys.* **474**, 653–664.

AN UNUSUAL QUADRUPLE SYSTEM  $\xi$  TAURI

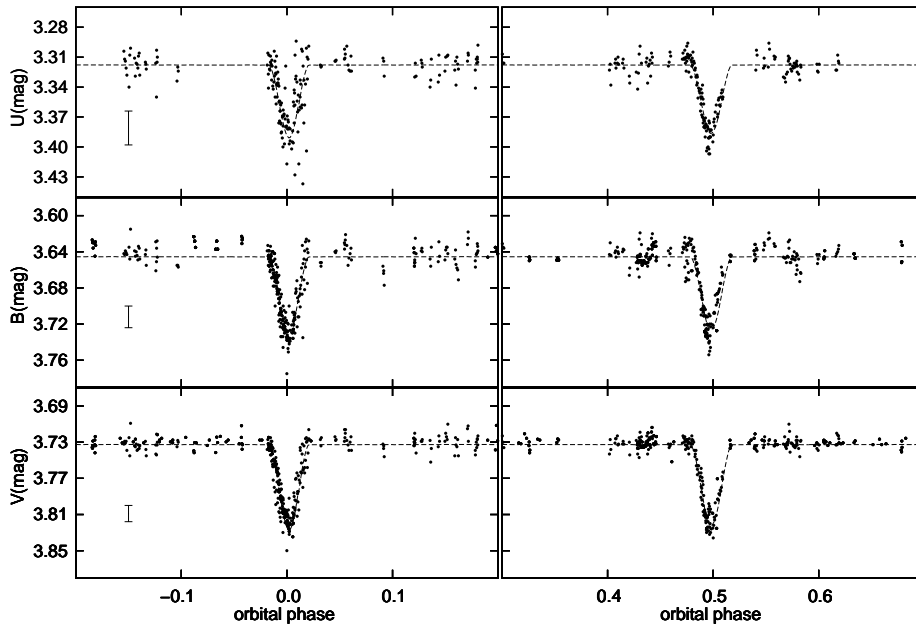


Figure 3: The *UB* light curves of  $\xi$  Tau Top panel: *U* filter, middle panel: *B* filter, bottom panel: *V* filter. Data sources (number of observations): Hvar Observatory (1308), SAAO (76), Hipparcos satellite (69), Villanova APT (401). Only minima and their close surroundings are shown. The shape of the light curves in regions which are not displayed is the same as it is in the surroundings of minima. The synthetic light curve is denoted by dashed line. The upper limit of the absolute uncertainty of one observation is denoted by line segments.